Proceedings of the 5th WSEAS Int. Conf. on SIGNAL, SPEECH and IMAGE PROCESSING, Corfu, Greece, August 17-19, 2005 (pp155-162)

Fractal Robustness and Parameter Tuning $PI^{\lambda}D^{\mu}$ Controllers

ABDELBAKI DJOUAMBI*, ABDELFATAH CHAREF and TAREK BOUKTIR***

* University Larbi Ben M'Hidi, Oum El-Bouaghi, Algeria

** University Mentouri, Ain El Bey, Constantine, Algeria

Abstract:- This paper presents a transposition of fractal robustness in automatics through the fractional order control and fractional feedback control of some of typical systems. Fractal robustness expresses the robustness of damping in nature, that fractality ensures through non integer derivation. This concept is illustrated by the relaxation of water on a porous dyke, its damping being independent of the motion of water mass. This robust phenomenon is paradoxical in the integer approach of mechanics, where any relaxation presents a damping linked to the carried mass. The considered dynamic model which governs this phenomenon is a non integer order linear differential equation where the natural frequency and the damping ration of the oscillatory mode of the solution are determined. Using such model as an open-loop reference model, a new tuning strategy of non integer order $PI^{\lambda}D^{\mu}$ controller has been presented for some typical systems. The performances of robustness is compared and illustrated with an ordinary PID controller through frequency and time responses.

Key-words:- fractal systems, fractional feedback control, tuning, robustness.

1 Introduction

As summarized in [1], [2] and [3], many real-world physical systems are well characterized by fractional order differential equations. In particular, it has been shown that the relaxation of water on a porous dyke can be more adequately molded by fractional order integrator [4]. The analyses seems to show that the relaxation is characterized by a natural frequency which depends on the motion water mass and by a damping ration which is independent of it.

Although it appears paradoxical in the integer approach of mechanics, where any relaxation presents a damping linked to the carried mass, this result reveals the insensitivity of the damping ration to a parameter at least. It therefore expresses the robustness of the stability degree of the relaxation phenomenon.

The aim of the following development consists in the transposition of such robustness in control systems through fractional order $PI^{\lambda}D^{\mu}$ controller using an elementary fractional order integrator as a reference model of the open-loop control system.

2 Fractal robustness

The concept of fractal robustness may be illustrated by the relaxation of water on a porous dyke, where the damping ration is independent of the mass of moving.

Given a mass M of water and the flow section S, considering the fractal character of the dyke porosity and the corresponding recursivity, it can be demonstrated that the pressure $P(t)$ at the water-dyke interface has the following differential equation [3]:

$$\frac{M}{S^2}\frac{1}{w_0^{\alpha-1}}\left(\frac{d}{dt}\right)^{\alpha} p(t) + p(t) = 0 \ , \qquad 1<\alpha<2 \qquad (1)$$

This equation represents the dynamic model of the water dyke interface.

Taking the Laplace transform of equation (1), we obtain:

$$(\tau s)^{\alpha} P(s) + P(s) = 0 \qquad (2)$$

Where

$$\tau = \left(\frac{M}{S^2 w_0^{\alpha-1}}\right)^{1/\alpha} \qquad (3)$$

This operational equation is translated by the functional diagram of Figure 1 which reminds that of a free control loop ($E(s)=0$). Because of a unit feedback, the direct chain determines an open loop transmittance of the form:

$$\beta(s) = \left(\frac{1}{\tau s}\right)^{\alpha} = \left(\frac{w_u}{s}\right)^{\alpha} \qquad (4)$$

which is just the transmittance of a non integer integrator whose unit gain frequency is $w_u = 1/\tau$.

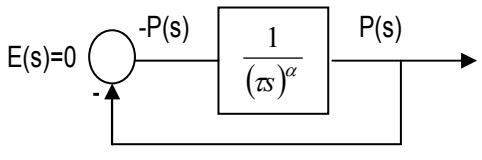

Fig.1 Functional diagram making it possible to define an open loop transfer.

Given that $\arg\beta(jw) = -\alpha\frac{\pi}{2}$ with $1<\alpha<2$, the Nichols locus of $\beta(jw)$ is a vertical straight line abscissa between $-\pi/2$ and $-\pi$.

When water mass M changes, frequency w_u is modified in conformity with the relation

$$w_u = \left(w_0^{\alpha-1} \frac{S^2}{M} \right)^{1/\alpha} \quad (5)$$

So, the template slides on itself at the time of variation of the water mass. Such a vertical displacement of a variation of the template ensures the constancy of phase margin ϕ_m (Figure 2). This expresses the robustness of stability degree.

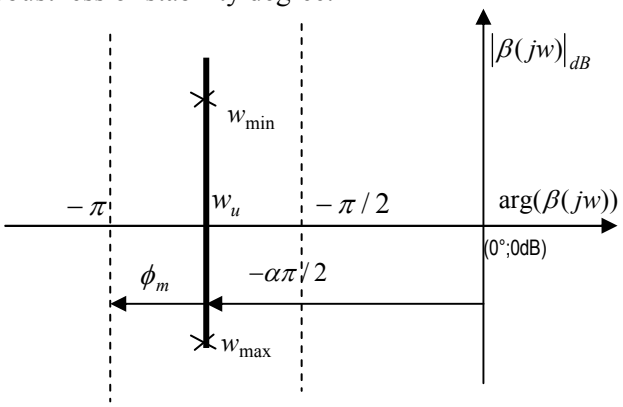

Fig. 2 Illustration of fractal robustness.

In controller design, the objective is to achieve such a similar frequency behavior, in a medium frequency range around w_u, knowing that the closed loop dynamic behavior is exclusively linked to the open loop behavior around w_u. Therefore, the ideal controller design comprises:

- an open loop Nichols locus which forms a vertical straight line segment around w_u for the nominal parametric state of plant,
- and a sliding of template on itself when there exist parameter change in plant.

The search for the synthesis of such a template defines the non integer approach that the second generation CRONE control uses [5].

3 Elementary fractional Order control

In this section we present the fundamental characteristics of an elemental control system with an open-loop transfer function given by a fractional order integrator. Based on this study, in the next section it is developed a tuning method for $PI^{\lambda}D^{\mu}$ controller for some of typical plants.

Let us consider the unit feedback system represented in Figure 3 with open-loop transfer function

$$G(s) = \frac{K}{s^m} \quad , \quad s=jw, \quad (1<m<2) \quad (6)$$

3.1 Frequency domain characteristics

The open-loop Bode diagrams of amplitude and phase shown in figure 4 have a slope of $-20m$ *dB/dec* and a constant phase of $-m\pi/2$ *rad*. Therefore, the closed-loop system has a constant phase margin of:

$$\phi_m = (1-\frac{m}{2})\pi \ \ (rad) \quad (7)$$

that is independent of the gain K.

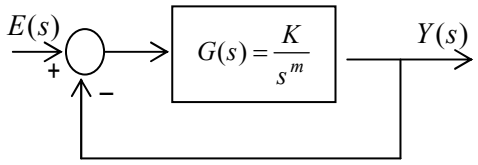

Fig.3 Elemental control system with fractional order integrator ($1< m <2$).

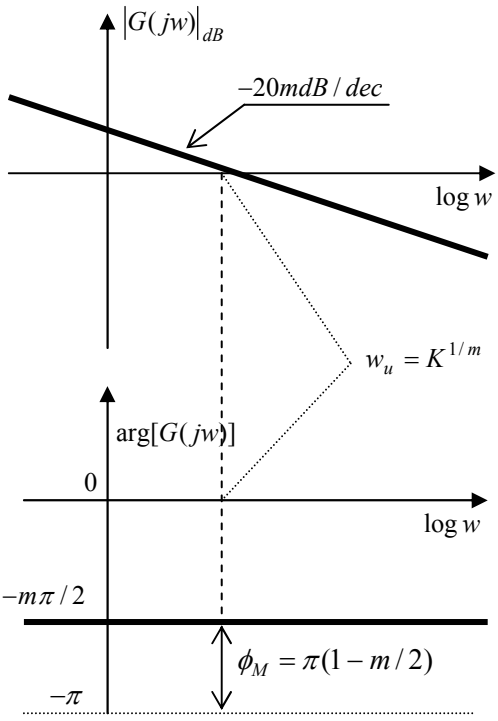

Fig. 4 Open-loop Bode diagram of G(s), ($1< m <2$).

Consider now H(s), the closed-loop transfer function of the unit feedback system presented in figure 3:

$$H(s) = \frac{Y(s)}{E(s)} = \frac{G(s)}{1+G(s)} = \frac{1}{(s/wu)^m + 1} \quad (8)$$

where $w_u = k^{1/m}$ denotes the open-loop crossover frequency. The asymptotic approximation of equation (8) indicates that the magnitude (phase) asymptotically approaches a horizontal straight line at *0 db* and *(0 rad)* as $w/w_u \to 0$ and a straight line of $-20m$ *dB/dec* ($-m\pi/2$ rad) as $w/w_u \to \infty$.

The resonance peak M_r and the frequency at which occurs w_r are given by the formulae [6]:

$$M_r = \frac{1}{\sin(m\pi/2)} \tag{9}$$

$$w_r = w_u \left|\cos(m\pi/2)\right|^{1/m} \tag{10}$$

3.2 Time domain characteristics

Fractional order systems have an infinite dimension [7]. Proper approximation by finite difference equation is needed. Specifications for a control system design often involve certain requirement associated with the time response. Hence, for the purpose of time domain analysis, synthesis and simulations, the need arises for a rational function approximation [8] and [9].

The asymptotic behavior with slope of *-20m dB/dec* of the function (6) is approximated by a number of zig-zag lines connected together with alternate slopes as represented in figure 5:

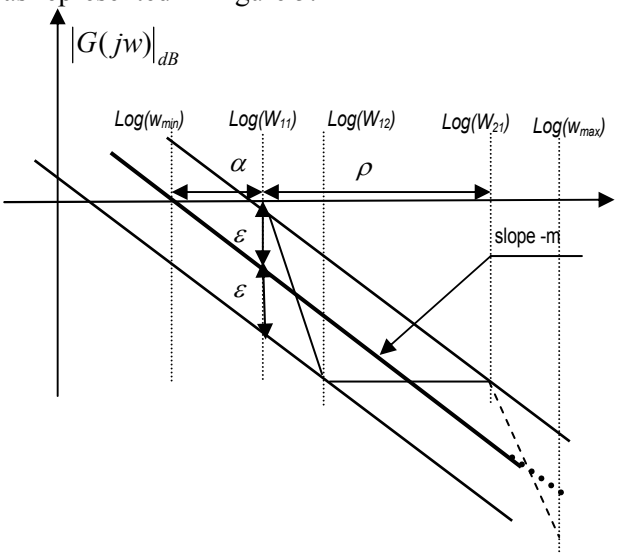

Fig 5 Broken-line approximation of *G(s)*

where ε denotes the approximation error,

$$\rho = \frac{2\varepsilon}{(1-m)m}, \quad \alpha = \frac{\varepsilon}{m} \tag{11}$$

Given a frequency band of interest $[w_{\min}, w_{\max}]$, the approximated function of *G(s)* can be expressed by the following equation:

$$G(jw) = \frac{1}{(w/w_u)^m} \approx \frac{1}{w_{\min}^m} \frac{\prod_{i=1}^{N}(1+jw/w_{i2})}{\prod_{i=1}^{N}(1+jw/w_{i1})} \tag{12}$$

where $w_{1,1} = w_{\min}10^{\alpha}$ and $w_{1,2} = w_{1,1}10^{\rho m}$.

for $i \geq 2$

$$w_{i,1} = 10^{\rho} w_{i-1,1}, \qquad w_{i,2} = w_{i,1}10^{\rho m}. \tag{13}$$

Given an approximation error ε, the number of cells N is obtained by the following equation:

$$N = E\left\{\begin{matrix} \frac{m(1-m)}{2\varepsilon}\left[\log_{10}(w_{\max}) - \log_{10}(w_{\min})\right] \\ -\frac{1-m}{2} \end{matrix}\right\} + 1, \tag{14}$$

Using equation (8) and equation (12) the closed loop approximated transfer function is presented by the following equation:

$$H(jw) \approx \frac{\prod_{i=1}^{N}(1+jw/w_{i2})}{w_{\min}^m \prod_{i=1}^{N}(1+jw/w_{i1}) + \prod_{i=1}^{N}(1+jw/w_{i2})}, \tag{15}$$

Figures 6 and 7 present the frequency response of the ideal function and that of its approximation with *N=10, m=1.5* and frequency band *[10^{-6},10^{6}]*. The figures show that the two curves are overlapping. Taking the Laplace inverse transform of equation (15), the time responses of the considered closed loop system for *m*=(1.1, 1.5, 1.9) and *N=10* is presented in figure 8.

Figure 9 shows the step responses of the closed loop system for different values of the system gain k with *m=1.5*. It can be seen that the first overshoot remains constant, showing a robustness that characterizes the considered fractional system.

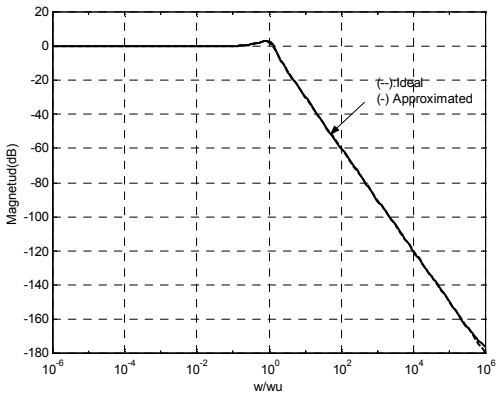

Fig. 6 Magnitude plot of the ideal system and its approximation

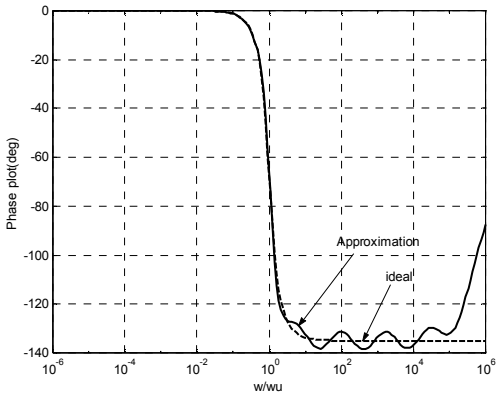

Fig. 7 Phase plot of the ideal system and its approximation

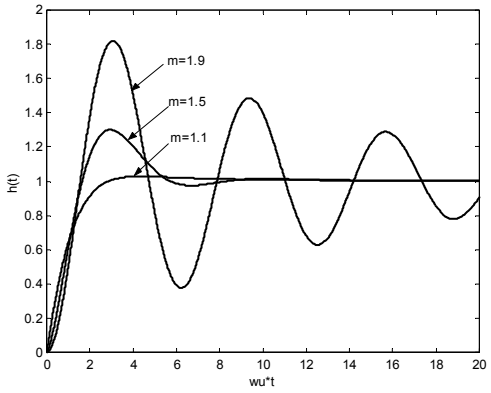

Fig. 8. Step response of the closed-loop system for different values of m.

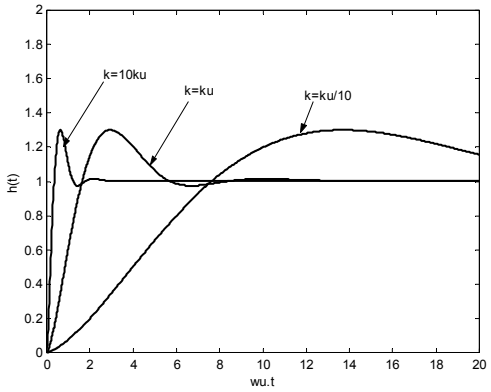

Fig. 9. Step response of the closed-loop system for different values of system gain K.

The percent overshoot $M_p(\%)$ versus m (Figure 10) can be approximated by the expressions:

$$M_p = \frac{h_{\max} - h(\infty)}{h(\infty)} \qquad (16)$$

$$M_p \approx 0.8(m-1)(m-0.75), \quad 1<m<2 \qquad (17)$$

the peak time T_p (Fig.11) and the rise time T_r (Fig.12) of the unit step response are given by the approximate formulas:

$$w_u T_p \approx \frac{1.1057(m-0.2546)^2}{(m-0.9205)}, \qquad 1<m<2 \qquad (18)$$

$$w_u T_r \approx \frac{0.1306(m+1.1607)^2}{(m-0.7035)}, \qquad 1<m<2 \qquad (19)$$

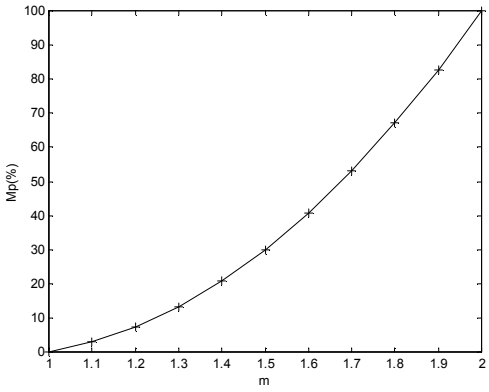

Fig. 10 Percent overshoot versus order m.

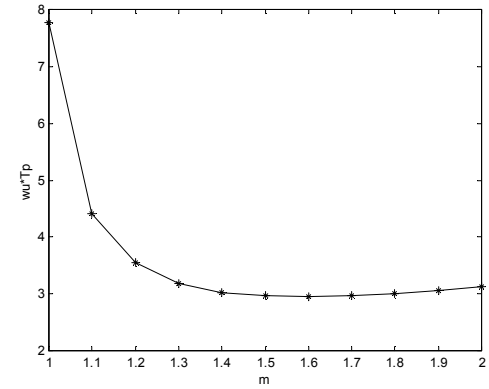

Fig. 11 Normalized peak time versus order m

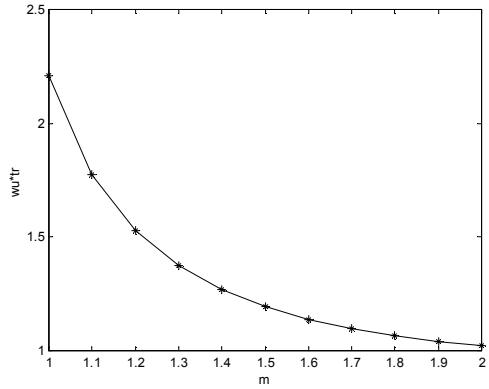

Fig. 12 Normalized rise time versus order m

4 Tuning method of PI$^{\lambda}$D$^{\mu}$ controllers

We have established a simple design of an elementary fractional order control system based on the parameters m and w_u. Therefore, in this section we address the Fractional Order Integrator of equation (6) as reference function $G_m(s)$ for PI$^{\lambda}$D$^{\mu}$ control system. We start by considering the closed-loop system shown in fig.13, where $C(s)$ is *the* PI$^{\lambda}$D$^{\mu}$ controller and $G_p(s)$ the plant transfer function characterized by an asymptotic order at low frequency $0 \le n' \le 2$ and at high frequency $2 \le n \le 4$ with $n' < n$ (figure 14).

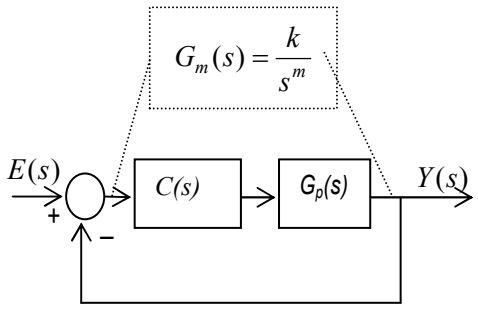

Fig. 13. Feedback control system with $PI^{\lambda}D^{\mu}$ controller.

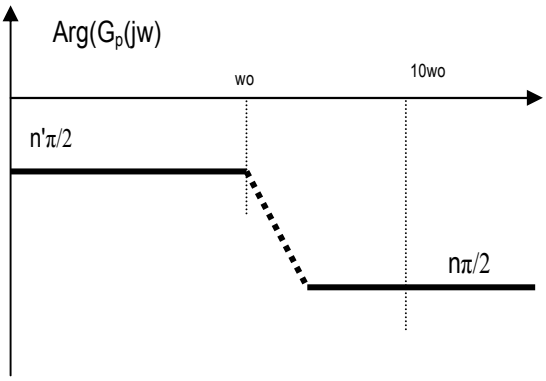

Fig. 14 Asymptotic phase plot of the considered plant $G_p(s)$

The ideal transfer function of a $PI^{\lambda}D^{\mu}$ controller has the following form:

$$C(s) = K_p(1 + \frac{T_i}{s^{\lambda}} + T_d s^{\mu}) \tag{20}$$

Where λ and μ are positive real numbers, K_p is the proportional gain, T_i the integral constant and T_d the differential constant.

The crossover frequency w_u is considered to be superior than 10 times the transitional frequency of the plant.

The reference open-loop transfer function has transfer function:

$$G_m(s) = \frac{1}{(s/w_u)^m} \tag{21}$$

where w_u and m are fixed according to the desired closed-loop performances.

The tuning method of the $PI^{\lambda}D^{\mu}$ is based on the interpretation of the open-loop transfer function $T(s)$ which can be written as:

$$T(s) = C(s)G_p(s) \tag{22}$$

The transmittance $T(s)$ can here be considered to be on approximation of the open loop transfer function $G_m(s)$, then we can write:

$$K_p(1 + \frac{T_i}{s^{\lambda}} + T_d s^{\mu})G_p(s) \approx \frac{K_u}{(s)^m} \tag{23}$$

where $K_u = w_u^m$.

Given a frequency band of interest:

$$w_{min} << 10w_0 < w_u << w_{max},$$

where, w_0 denotes the transitional frequency of the plant, the transmittance $T(s)$ should presents:

- an asymptotic slope of $-20m$ dB/dec at low and high frequency of the limited bandwidth $[w_{min}, w_{max}]$ which allows to calculate the parameters λ and μ.
- the same magnitude with the reference $G_m(s)$ in the high and low frequency, so, the initial values of parameters T_i' and T_d' can be estimated with an initial value of K_p considered to be $K_p = 1$.
- a crossover frequency equal to w_u, the parameter K_p can be deduced using the initial values T_i' and T_d'.
- finally: adjusting the parameters T_i' an T_d' to be :

$$T_i = K_p T_i' \text{ and } T_d = K_p T_d'.$$

Taking n and n' as the asymptotic order of the plant $G_p(s)$ at high an low frequency respectively, the controller parameters can be given by the following equations:

$$\mu = n - m, \ \lambda = m - n', \tag{24}$$

$$T_d' = \frac{K_u}{|G_p(jw_{\max})| w_{\max}^n}, \tag{25}$$

$$T_i' = \frac{K_u}{|G_p(jw_{\max})| w_{\min}^{n'}}, \tag{26}$$

$$K_p = \frac{|G_p(jw_u)|}{|1 + T_i'(jw_u)^{-\lambda} + T_d'(jw_u)^{\mu}|} \tag{27}$$

$$T_i = T_i' K_p \text{ and } T_d = T_d' K_p \tag{28}$$

5 Simulation results

In these section we analyze the open-loop frequency and closed-loop time response characteristics of the $PI^{\lambda}D^{\mu}$ system tuned according to the reference design parameters (m, w_u).

In order to establish different case studies, we adopt three distinct processes, given by:

$$G_{p1} = \frac{g_0}{(s/w_0)^2 + 2\varepsilon(s/w_0) + 1} \tag{39}$$

$$G_{p2} = \frac{g_0}{\frac{s}{w_1}(1 + \frac{s}{w_0})} \tag{30}$$

$$G_{p3} = \frac{g_0}{\frac{s}{w_1}(1 + \frac{s}{w0})^2} \tag{31}$$

Given a frequency band of interest: $[10^{-6},10^{6}]$ *rad/sec* and the parameter values of the above plants as follow:

- plant $G_{p1}(s)$: $g_0 = 10$, $w_0=33.33$ *rd/s* and $\varepsilon = 0.01$.
- plant $G_{p2}(s)$: $g_0 = 1$, $w_0=50$ *rd/s and* $w_1 =16.89$ *rd/s*.
- plant $G_{p3}(s)$: $g_0 = 1$, $w_0=10$ *rd/s and* $w_1=17$ *rd/s*.

From the desired closed-loop performances we can fix the order m and the crossover w_u of the reference model (Sec. 3).

The reference model and $PI^{\lambda}D^{\mu}$ closed-loop system are simulated in time domain by use of equation (12) with $N=10$.

In order to check the achieved approximation in frequency domain we present in Fig. 15, 16, 17, 18, 19 and 20 the Bode diagrams of amplitudes and phases for the reference model $G_m(s)$ and $PI^{\lambda}D^{\mu}$ open-loop systems of $G_{p1}(s)$, $G_{p2}(s)$ and $G_{p3}(s)$ with the reference model design parameters $\phi_m = 45^{\circ}$ and $w_u=500$ *rad/s.* This tuning corresponds to m=1.5. We see that the curves are very similar in both cases.

Figures 21, 22 and 23 present the step response of the reference model and the $PI^{\lambda}D^{\mu}$ closed-loop systems with the previous case. The figures show that the curves are very similar.

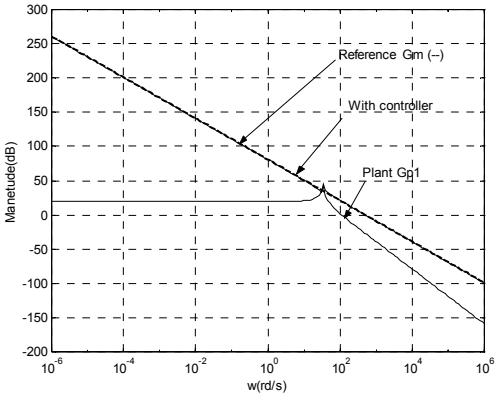

Fig.15 Magnitude plot of the reference model and $PI^{\lambda}D^{\mu}$ open-loop system for $G_{p1}(s)$.

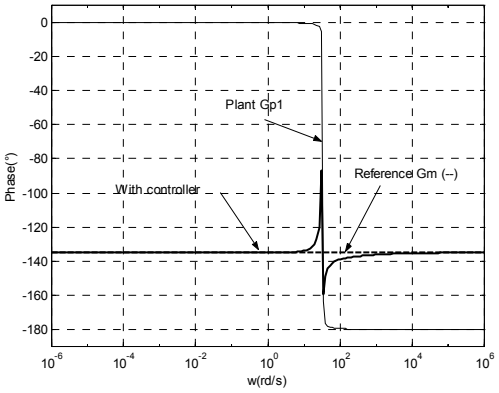

Fig.16 Phase plot of the reference model and $PI^{\lambda}D^{\mu}$ open-loop system for $G_{p1}(s)$.

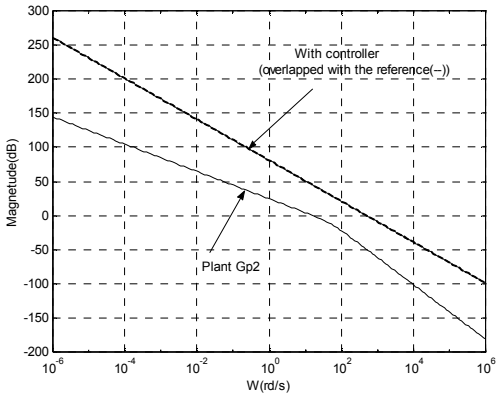

Fig.17 Magnitude plot of the reference model and $PI^{\lambda}D^{\mu}$ open-loop system for $G_{p2}(s)$.

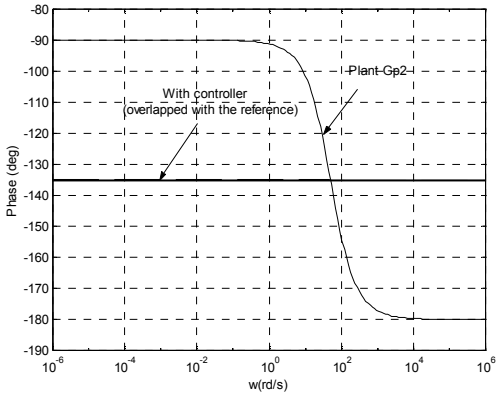

Fig.18 Phase plot of the reference model and $PI^{\lambda}D^{\mu}$ open-loop system for $G_{p2}(s)$.

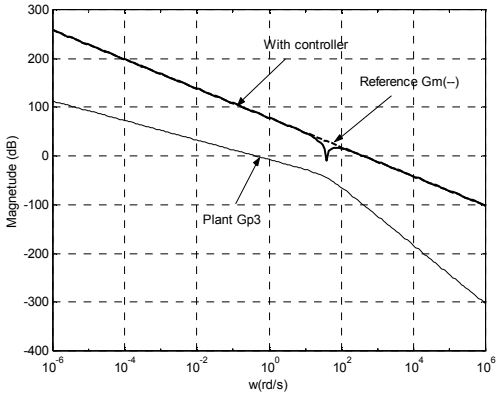

Fig.19 Magnitude plot of the reference model and $PI^{\lambda}D^{\mu}$ loop system for $G_{p3}(s)$.

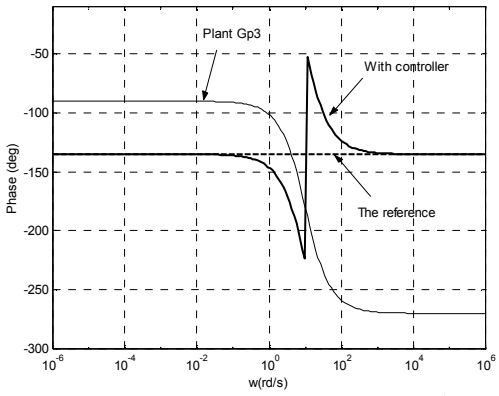

Fig.20 Phase plot of the reference model and $PI^{\lambda}D^{\mu}$ open-loop System for $G_{p3}(s)$.

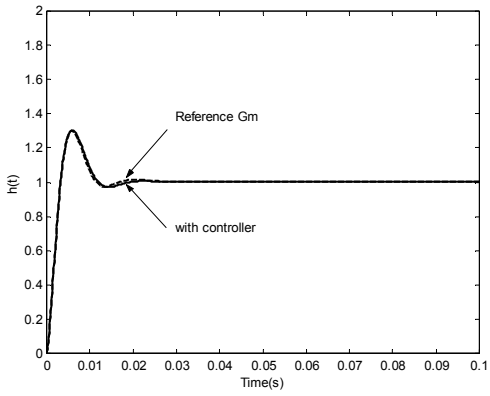

Fig.21 Step response of the reference model and $PI^{\lambda}D^{\mu}$ closed-loop system for $G_{p1}(s)$.

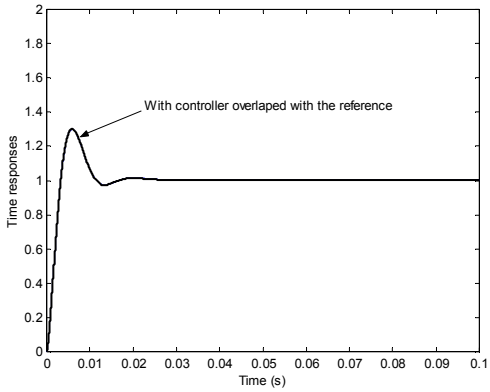

Fig. 22 Step response of the reference model and $PI^{\lambda}D^{\mu}$ closed-loop system for $G_{p2}(s)$.

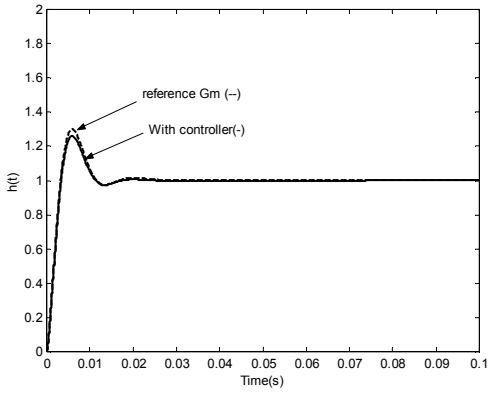

Fig.23 Step response of the reference model and $PI^{\lambda}D^{\mu}$ closed-loop system for $G_{p3}(s)$.

6 Performances

In this section we present a comparative study of the robustness performances obtained with the $PI^{\lambda}D^{\mu}$ controller and a classical type *PID* controller.

The plant is a second order system given by the following transfer function:

$$G(s) = \frac{g_0}{\frac{s^2}{w_0^2} + 2\varepsilon\frac{s}{w_0} + 1} \tag{32}$$

where g_0 denotes the static gain, w_0 the transitional frequency and ε the damping ration.

The nominal values of the parameters g_0, w_0 and ε are given as follow:

$$g_0 = 10,\ w_0 = 33.33 \text{ and } \varepsilon = 0.01. \tag{33}$$

In order to achieve the robustness propriety of each controller, the values of g_0 and w_0 are modified as follow:

$$g_{0\min} = \frac{g_0}{10};\ g_{0\max} = 10g_0 .$$

$$w_{0\min} = \frac{w_0}{2};\ w_{0\max} = 2w_0 . \tag{34}$$

the fractional controller $PI^{\lambda}D^{\mu}$ and classical type *PID* are calculated for the considering plant under the nominal values of equation (33) and the desired closed-loop frequencies specifications given as follow:

$$\phi_m = 45°, \text{ and } w_u = 500 . \tag{35}$$

The transfer function of a classical *PID* controller has the following form:

$$c_c(s) = c_0\frac{(1+s/z_1)(1+s/z_2)}{(1+s/p_1)(1+s/p_2)} \tag{36}$$

in which:

$$c_0 = 50.797;\ z_1 = 3.7796 \text{ rd/s}; z_2 = 188.982 \text{ rd/s};$$
$$p_1 = 0.6299 \text{ rd/s}; p_2 = 1322.90 \text{ rd/s}.$$

The transfer function of a fractional $PI^{\lambda}D^{\mu}$ controller has the following form:

$$C(s) = K_p(1 + \frac{T_i}{s^{\lambda}} + T_d s^{\mu}) \tag{37}$$

using equations (24,…,28) :

$$K_p = 0.97;\ T_i = 1083.30;\ T_d = 0.9752;$$
$$\lambda = 1.5;\ \mu = 0.5 .$$

As shown in Figure 24 and figure 25, fractional order $PI^{\lambda}D^{\mu}$ controller realizes better robustness versus static gain plant variation with smaller overshot and fastest rise time. Figure 26 gives the step responses of the $PI^{\lambda}D^{\mu}$ control system with different values of w_0, compared to the step responses of the classical type *PID* control system (Figure 27) with the same variation of w_0, it can be shown that fractional order $PI^{\lambda}D^{\mu}$ controller realizes better robustness against plants parameters variation

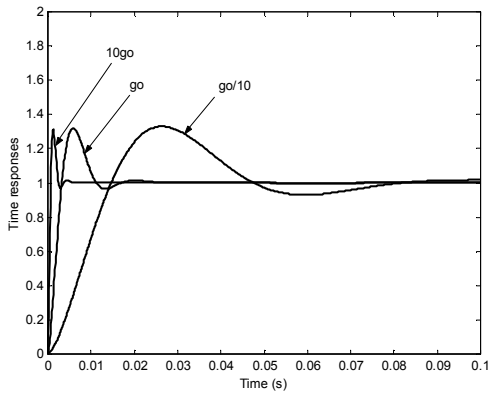

Fig. 24 Step response of the closed-loop system with $PI^{\lambda}D^{\mu}$ controller for different values of g_0.

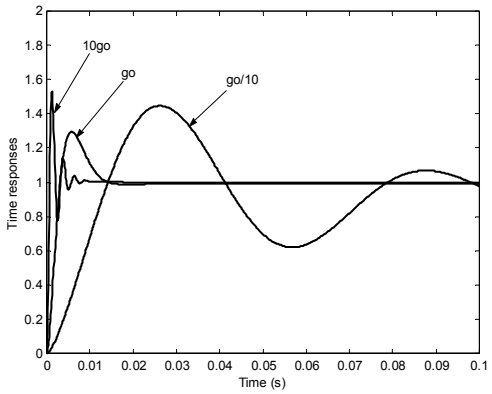

Fig. 25 Step response of the closed-loop system with classical *PID* controller for different values of g_0.

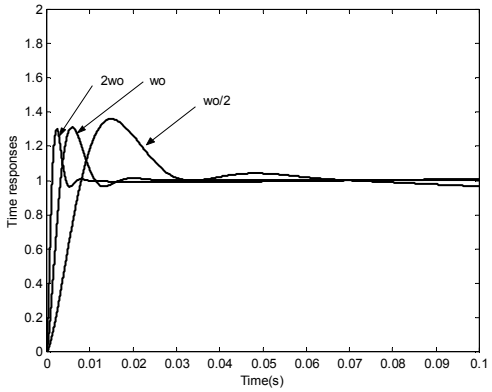

Fig. 26 Step response of the closed-loop system with $PI^{\lambda}D^{\mu}$ controller for different values of w_0.

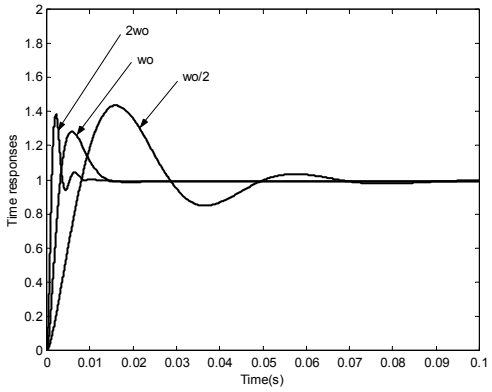

Fig.27 step response of the closed-loop system with classical *PID* controller for different values of w_0.

7 Conclusion

In this paper, an alternative point of view for the tuning of robust fractional $PI^{\lambda}D^{\mu}$ controller has been presented. The synthesis method is based on the interpretation of the open loop $PI^{\lambda}D^{\mu}$ control system witch can be considered to be of an elementary fractional order integrator model, Such model governs the relaxation of water on porous dyke, it consists in a differential equation of non integer order between 1 and 2. Damping is indeed specific to the non integer of differential equation imposed by the fractal dimension of the dyke. This expresses a remarkable property: fractality determines damping in nature. The robustness of damping is illustrated by a frequency template in the Nichol's plane whose form and vertical sliding ensure the invariance of the phase margin.

An intuitive broken-line approximate synthesis method of frequency-band controllers is also introduced which has a satisfactory accuracy in frequency domain.

The experimental results with several typically plants show the robustness of proposed fractional $PI^{\lambda}D^{\mu}$ control system compared to a classical PID controller.

8 References

[1] P.J. Tovik and R. T. Bagley, "*On the appearance of the fractional derivative in the behavior of real materials*," Transaction of the ASME, vol. 51, N°.6 1984, pp. 294-298;

[2] Van Der Ziel., "*Unified presentation of 1/f noise in electronic devices: fundamental 1/f noise sources*", Proceedings of IEEE, Vol 76, 1988, pp 233-258.

[3] A. Oustaloup, F. levron, and B. Mathieu, "*Frequency-band complex non integer differentiator: Characterization and synthesis"* IEEE Trans. Circuit Syst. I., vol. 47, 2000, pp. 25-39.

[4] A. Oustaloup, X. Moreau and M. Nouillant, "*From fractal robustness to non integer approach in vibration insulation: the CRONE suspension*" Proceeding of 36th Conference on Decision and control, California, USA, 1997, pp. 4979-4984.

[5] A Oustaloup, "*La commande CRONE*" Edition Hermès, Paris, 1991.

[6] Ramiro S. Barbosa, J. A. Tenreiro Machado and Isabel M. Ferreira "*A Fractional Calculus Perspective of PID Tuning*" Proceedings of DETC.03ASME 2003 Design Engineering Technical Conferences and Computers and Information in Engineering Conference Chicago, Illinois, USA, September 2-6, 2003

[7] A. Scotti and S. G. Meneveau, "*Fractal dimension of velocity signals in high- Reynolds-numbers hydrodynamic turbulence",* Physical Review, vol 51, N° 6, 1995, pp. 5594-5608.

[8] A. Charef, H. H. Sun, Y. Y. Tsao, and B. Onaral, "*Fractal Systems as Represented by Singularity Function*" IEEE Trans. Vol. 37, No. 9, 1992, pp. 1465-1470.

[9] A. Djouambi and A. Charef "*Approximation optimale et synthèse d'un model d'ordre non entier," Proceeding of 1th International Conference on Electrical systems PCSE'05, Algéria, 2005, pp.370-374.*